# Polarized photovoltage spectroscopy study of InAs∕GaAs ( 001 ) quantum dot ensembles

Jayeeta Bhattacharyya, Sandip Ghosh, Stefan Malzer, G. H. Döhler, and B. M. Arora

---

---

# Polarized photovoltage spectroscopy study of InAs/GaAs(001) quantum dot ensembles

Jayeeta Bhattacharyya and Sandip Ghosh[a)]
*Department of Condensed Matter Physics and Material Science, Tata Institute of Fundamental Research, Homi Bhabha Road, Mumbai 400005, India*

Stefan Malzer and G. H. Döhler
*Max Planck Research Group, Institute of Optics, Information and Photonics, University of Erlangen-Nuremberg, Günther-Scharowsky-Str. 1, Bau 24, 91058 Erlangen, Germany*

B. M. Arora
*Department of Condensed Matter Physics and Material Science, Tata Institute of Fundamental Research, Homi Bhabha Road, Mumbai 400005, India*

We have studied self-assembled InAs quantum dot (QD) ensembles on GaAs(001) substrate using polarized photovoltage spectroscopy. The photovoltage spectrum shows four prominent QD related features whose nature differs for probe light incident along [001] and polarized parallel to [110] and [1$\bar{1}$0] directions. The polarization anisotropy suggests that for the lowest energy transition there is only a change in the oscillator strength with change in polarization, while for the higher energy transitions there is also an apparent shift in the transition energy. By comparison with simulations of the absorption spectrum, we show that the main features of the observed polarization anisotropy can be understood on the basis of a model where an anisotropic two dimensional harmonic oscillator potential represents the lateral confinement of the carriers within the QD in the (001) plane. © *2005 American Institute of Physics*. [DOI: 10.1063/1.2132533]

Among the several interesting consequences of quantum confinement in III–V semiconductor nanostructures is the appearance of optical polarization anisotropy in systems whose underlying crystal structure has high symmetry. In self-assembled InAs quantum dots (QDs) on GaAs(001) substrates, one observes a difference between the [1$\bar{1}$0] and [110] polarizations of the photoluminescence (PL) yield normal to the (001) plane. This is not expected in bulk crystals with zinc blende structure. This anisotropy is important for optoelectronic device applications, for example in fixing the polarization of surface emitting lasers[1] and making polarization sensitive photodetectors.[2] Several microscopic origins of QD potential anisotropy that can result in such optical polarization anisotropy have been suggested. They include anisotropic shape[1,3] and In/Ga distribution.[4] The latter may be enhanced upon capping with GaAs due to anisotropic interdiffusion of In/Ga.[5] Varying strain[6] within the QD and consequent valence band mixing[7,8] can also give rise to in-plane optical anisotropy. A combination of strain and piezoelectric effect has also been shown to be important.[9–11] Through PL studies on single QDs, both shape[12] and electron-hole exchange interaction[13] have been suggested as the source of polarization anisotropy in InP/Ga$_{0.5}$In$_{0.5}$P(001) QDs and planar electric fields[14] for InAs/GaAs(001) QDs. Here we focus on an ensemble of such QDs.

Previous studies of optical polarization anisotropy in InAs QDs have all relied on PL. In PL, which usually requires low temperatures, information about the true density of states is masked by the excess carrier capture/transfer/population statistics, and emission is dominated by low energy transitions. Here we report polarized photovoltage (PV)

spectroscopy measurements. With PV one directly obtains the absorption ($\alpha_{QD}$) spectrum up to the highest confined QD levels,[15] at room temperature. Microscopic origins of the potential anisotropy are difficult to quantify and their inclusion requires involved calculations, while a phenomenological model is more useful for device characteristics simulation. We have simulated $\alpha_{QD}$ using a model where an anisotropic two-dimensional (2D) harmonic oscillator (HO) potential determines carrier confinement in the (001) plane and compared it with the observed polarization anisotropy.

InAs QDs were grown via Stranski-Krastanow growth mode on $p^+$ GaAs(001) substrate at 490 °C using molecular-beam epitaxy. The samples had two InAs QD layers (~2 monolayer nominal thickness) separated by 50 nm and placed within the *i*-GaAs region (850 nm) of a *n-i-p* structure. Atomic force microscope (AFM) pictures of the QDs without the top GaAs cap, reveal an average height of 9 nm, width of 40 nm and density of $2 \times 10^{10}$ cm$^{-2}$. Such QDs are known to have small elongation (~10%) along [1$\bar{1}$0][1,5,14] and we too observed a small shape asymmetry but due to the poor in-plane resolution of AFM we could not exactly quantify the asymmetry. Optical polarization anisotropy was measurable only in samples with narrow QD height distribution, typically ≤5% of mean. PV measurements were performed in the soft contact mode,[16] with the samples placed between a transparent indium-tin-oxide coated glass and a copper electrode. The probe beam was light from a 100 W tungsten lamp dispersed by a grating monochromator (1 meV band-pass), polarized with a Glan-Taylor prism and mechanically chopped at 23 Hz for phase sensitive detection. The samples were mounted with the cleaved edges, which are parallel to [110] and [1$\bar{1}$0], aligned at ±45° to the monochromator slit height (vertical) direction [Fig. 1(a) inset] and the polariza-
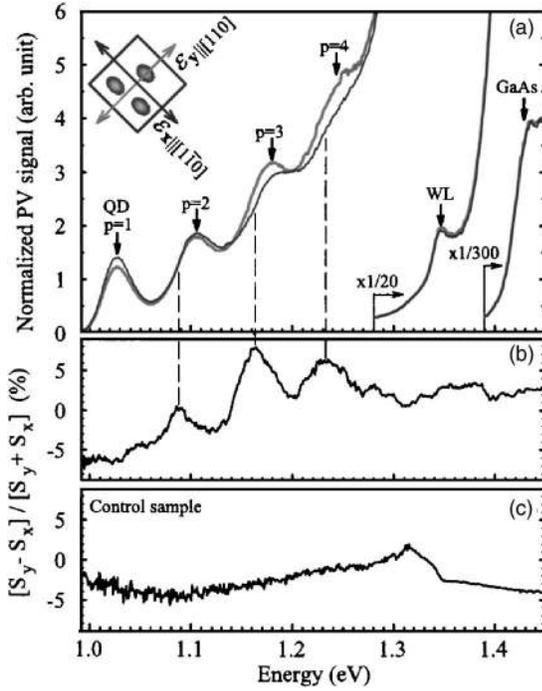
[a)]Electronic mail: sangho10@tifr.res.in

FIG. 1. (a) PV signal $S_x, S_y$ at 297 K from an InAs QD sample on GaAs(001), for probe light incident along $[001]\|\hat{\mathbf{z}}$, and polarized along $[1\bar{1}0]\|\hat{\mathbf{x}}$ (black line), and for $[110]\|\hat{\mathbf{y}}$ (gray line) directions, respectively. The inset is a schematic of the sample orientation during measurement. (b) Polarization anisotropy plot of the PV signal from the QD sample. (c) Polarization anisotropy plot of the PV signal from a control sample ($\text{In}_{0.65}\text{Ga}_{0.35}\text{As}/\text{InP}(001)$ quantum well), where anisotropy is absent.
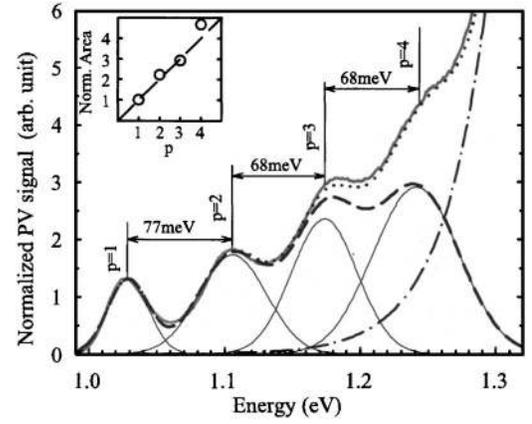
FIG. 2. The measured unpolarized PV spectrum (gray continuous line) and the fitted line shape (dotted line). The fitting function had four Gaussians (thin continuous lines) whose sum (thick dashed line) represents the total InAs QD contribution, plus an Urbach tail contribution (dash-dot line) from the InAs WL. The inset shows the variation of the area of the gaussians with peak index $p$, normalized to the area of the first ($p=1$). The dashed line (slope=1, intercept=0) is a guide for the eye.

tion axis was changed from 45° to −45°. This minimizes the errors, due to the usually large difference in the throughput for light polarization ‖ and ⊥ to the vertical direction.

Figure 1(a) shows the room temperature PV signal $S_x$ and $S_y$ from a QD sample for light incident along $[001]\|\hat{\mathbf{z}}$ and polarized with electric field vector $\mathcal{E}\hat{\mathbf{e}}\|[1\bar{1}0]\|\hat{\mathbf{x}}$ and $\mathcal{E}\hat{\mathbf{e}}\|[110]\|\hat{\mathbf{y}}$ directions, respectively. The peaks at lower energies labeled $p=1$–4 are identified with inhomogeneously broadened QD transitions. A feature due to the InAs wetting layer (WL) at 1.347 eV (theoretically calculated value ∼1.348 eV), and one due to the GaAs barrier, are also seen. The polarization anisotropy, defined as $[S_y - S_x]/[S_y + S_x]$, is plotted in Fig. 1(b). To test for errors we did measurements on $\text{In}_{0.65}\text{Ga}_{0.35}\text{As}/\text{InP}(001)$ quantum wells [Fig. 1(c)]. This control sample has no prominent features in the energy range where the anisotropy related features are seen in the QD sample. In the QD sample we find that at energies around the $p=1$ peak, there is a near constant negative anisotropy while at higher energies there are peaked features. However, the peaks in the anisotropy plot do not coincide in energy with peaks of the PV spectrum in Fig. 1(a), and instead arise in between the latter peaks (see vertical dashed line). These energy derivative-like features seem to suggest polarization dependent transition energy shifts. To understand the origins of such anisotropy we simulated $\alpha_{\text{QD}}$ as follows.

Within the effective-mass envelope wave function approximation, we consider the carrier confinement potential of the QD to be represented by a rectangular well along $\hat{\mathbf{z}}$ and a parabolic 2D-HO potential in the $\hat{\mathbf{x}}$-$\hat{\mathbf{y}}$ plane.[17] Since the QD height is much smaller than its lateral dimensions, the confinement energy for motion ‖$\hat{\mathbf{z}}$ and ⊥$\hat{\mathbf{z}}$ can be calculated separately under the adiabatic approximation.[18] The absorp-

tion spectrum is expected to be dominated by heavy-hole transitions. The transitions occur from valence band states labeled $\{l^v, m^v, n^v = 1\}$ to conduction band states $\{l^c, m^c, n^c = 1\}$, with energy

$$E_{lmn} = E'_g + \left(l + \tfrac{1}{2}\right)\hbar(\omega_x^c + \omega_x^v) + \left(m + \tfrac{1}{2}\right)\hbar(\omega_y^c + \omega_y^v) + \Delta E_{z,n=1}^c + \Delta E_{z,n=1}^v. \quad (1)$$

$E'_g$ represents the strained InAs heavy-hole band gap minus an effective exciton binding energy,[11] $\Delta E_z^c, \Delta E_z^v$ are the $\hat{\mathbf{z}}$ confinement energies. The oscillator frequency $\omega^c = \sqrt{fK_x/m_e^*}$, where $K_x$ is the spring constant defining the in-plane confinement potential along $\hat{\mathbf{x}}$, $f$ defines an effective band offset ratio for the in-plane potential and $m_e^*$ the electron effective mass and so on. In the first approximation with $K_x = K_y$, we can identify the $p=1$ peak with the {001} transition, $p=2$ with the two degenerate {101} and {011} transitions and so on. Figure 2 shows the unpolarized PV spectrum of the QDs fitted with a sum of four Gaussians representing the QD transitions plus an InAs WL related exponential Urbach tail. The Gaussians have nearly equal energy spacing as expected from the model and as is also seen in PL measurements.[19] The model also predicts an increase in $\alpha_{\text{QD}}$ proportional to $p$, arising from the degeneracy of the HO levels. PV measurements, unlike PL, can verify this and the inset of Fig. 2 shows that the relative area of the Gaussians, is nearly proportional to $p$. With these justifications for the 2D-HO potential model we next consider the anisotropic case where $K_y = \beta^2 K_x$, where $\beta$ is the anisotropy parameter. To calculate $\alpha_{\text{QD}}$ we need the oscillator strengths $\mathcal{O}$ for the transitions, and according to Kane's model[6,20]

$$\mathcal{O}_{lmn} \propto \frac{1}{2}\left(\frac{k_m^2 + k_n^2}{k^2}\hat{\mathbf{x}} + \frac{k_n^2 + k_l^2}{k^2}\hat{\mathbf{y}} + \frac{k_l^2 + k_m^2}{k^2}\hat{\mathbf{z}}\right)$$
$$\cdot \hat{\mathbf{e}}|P|^2 \delta_{l^c l^v}\delta_{m^c m^v}\delta_{n^c n^v}. \quad (2)$$

$P$ is the optical momentum matrix element. The delta functions determine the selection rules used. Here the wave vector $k$ components ($k_x = k_l$, $k_y = k_m$, $k_z = k_n$) for electrons are implicitly equal to those for holes. Our model therefore requires a shallow in-plane confinement potential for holes ($f$
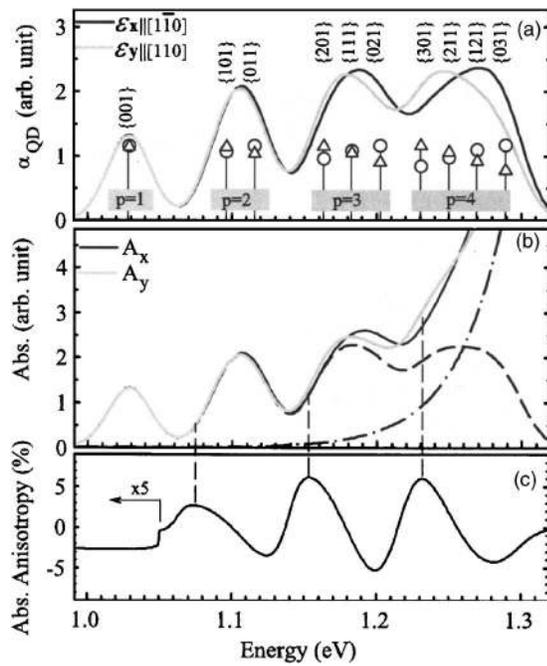
FIG. 3. (a) Simulated QD absorption spectrum for $\mathcal{E}\hat{x}\|[1\bar{1}0]$ (black line) and $\mathcal{E}\hat{y}\|[110]$ (gray line), with $\beta=1.29$. QD transitions are labeled and their energies are indicated (thin vertical lines), along with their relative oscillator strengths for $\mathcal{E}\hat{x}\|[1\bar{1}0]$ ($\mathcal{E}\hat{y}\|[110]$) by circles (triangles). (b) Simulated total absorption spectra $A_x$ and $A_y$, including the Urbach tail contribution (dash-dot line) from the InAs WL (same as that in Fig. 2), for $\mathcal{E}\hat{x}\|[1\bar{1}0]$ (black line) and $\mathcal{E}\hat{y}\|[110]$ (gray line), respectively. The total unpolarized $\alpha_{QD}$ is also shown (dashed line). (c) Simulated polarization anisotropy defined as $[A_y-A_x]/[A_y+A_x]$.

$\geq 0.9$). A shallow hole confinement potential is also suggested by capacitance-voltage measurements of Bock *et al.*[21] Using the $p=1$, 2 peak energies from experiment, and other relevant band structure information[22] we deduce the initial parameters keeping $\beta=1$. We then vary $\beta$, find the energies and the wave functions, and fit sinusoidal functions to the latter to estimate the $k$ components. $\alpha_{QD}$ line shapes were taken to be gaussians of width equal to that for the $p=1$ feature, and the overall magnitude was scaled to match the $p=1$ peak.

Figure 3(a) shows the simulated QD absorption spectra for $\mathcal{E}\hat{e}\|[1\bar{1}0]$ and for $\mathcal{E}\hat{e}\|[110]$ with $\beta=1.29$ which best matches our observations. The individual transitions are labeled and their energies and relative oscillator strengths are also shown. Figure 3(b) has the simulated total polarized absorption spectrum including the InAs WL and Fig. 3(c) shows the polarization anisotropy. We see that the main characteristics of the measured PV anisotropy spectrum, (i) a constant negative value around $p=1$ and (ii) peaked features at higher energy (with sharper rise than fall) arising in between peaks of the normal spectrum, are reproduced in the simulation. The overall magnitude of the anisotropy is also similar except for the absence of a rising background which possibly originates from the microscopic details of the potential and valence band mixing which are difficult to quantify. Thus the model shows that due to confinement potential anisotropy in the (001) plane, (i) the oscillator strength for the lowest non degenerate {001} transition changes with polarization and (ii) the degeneracy of the higher levels is lifted

and energy splitting occurs. The oscillator strengths of these higher energy transitions also vary with polarization in a regular fashion such that the net result for the ensemble manifests itself as an apparent shift in the transition energy [see Fig. 3(a)]. For $\beta=1.29$ the model predicts a lateral envelope wave function spread ($\sim 6\times$ the HO characteristic length scale $\sqrt{\hbar/\omega m^*}$) of 43 and 38 nm along $[1\bar{1}0]$ and $[110]$ direction, respectively, which is close to our measured average lateral QD dimensions.

In conclusion, optical polarization anisotropy [in the (001) plane] of self-assembled InAs QD ensembles on GaAs(001) substrate is an important property of this system with regard to optoelectronic device applications, especially surface emitting lasers. We showed that polarized PV spectroscopy is an ideal nondestructive tool for room temperature characterization of the anisotropy in the absorption spectrum of an ensemble of such QDs. Furthermore, we showed that the main characteristics of the optical polarization anisotropy can be explained on the basis of an anisotropy of the carrier confinement potential in the (001) plane, which can be modeled using an anisotropic 2D-HO potential.

[1]H. Saito, K. Nishi, S. Sugou, and Y. Sugimoto, Appl. Phys. Lett. **71**, 590 (1997).
[2]E. Greger, P. Riel, M. Moser, T. Kippenberg, P. Kiesel, and G. H. Döhler, Appl. Phys. Lett. **71**, 3245 (1997).
[3]M. Henini, S. Sanguinenetti, S. C. Fortina, E. Grilli, M. Guzzi, G. Panzarrini, L. C. Andreani, M. D. Upward, P. Moriarty, P. H. Beton, and L. Eaves, Phys. Rev. B **57**, R6815 (1998).
[4]J. Shumway, A. J. Williamson, A. Zunger, A. Passaseo, M. DeGiorgi, R. Cingolani, M. Catalano, and P. Crozier, Phys. Rev. B **64**, 125302 (2001).
[5]M. C. Xu, Y. Temko, T. Suzuki, and K. Jacobi, Surf. Sci. **580**, 30 (2005).
[6]S. Noda, T. Abe, and M. Tamura, Phys. Rev. B **58**, 7181 (1998).
[7]W. Yang, H. Lee, T. J. Johnson, P. C. Sercel, and A. G. Norman, Phys. Rev. B **61**, 2784 (2000).
[8]S. Cortez, O. Krebs, P. Voisin, and J. M. Gérard, Phys. Rev. B **63**, 233306 (2001).
[9]M. A. Migliorato, D. Powell, E. A. Zibik, L. R. Wilson, M. Fearn, J. H. Jefferson, M. J. Steer, M. Hopkinson, and A. G. Cullis, Physica E **26**, 436 (2005).
[10]O. Stier, M. Grundmann, and D. Bimberg, Phys. Rev. B **59**, 5688 (1999).
[11]L. Wang, J. Kim, and A. Zunger, Phys. Rev. B **59**, 5678 (1999).
[12]V. Zwiller, L. Jarlskog, M. E. Pistol, C. Pryor, P. Castrillo, W. Seifert, and L. Samuelson, Phys. Rev. B **63**, 233301 (2001).
[13]M. Sugisaki, H. W. Ren, S. V. Nair, K. Nishi, S. Sugou, T. Okuno, and Y. Masumoto, Phys. Rev. B **59**, R5300 (1999).
[14]I. Favero, G. Cassabois, A. Jankovic, R. Ferreira, C. Voisin, C. Delalande, Ph. Roussignol, A. Badolato, P. M. Petroff, and J. M. Gérard, Appl. Phys. Lett. **86**, 041904 (2005).
[15]B. Q. Sun, Z. D. Lu, D. S. Jiang, J. Q. Wu, Z. Y. Xu, Y. Q. Wang, J. N. Wang, and W. K. Ge, Appl. Phys. Lett. **73**, 2657 (1998).
[16]S. Datta, S. Ghosh, and B. M. Arora, Rev. Sci. Instrum. **72**, 177 (2001).
[17]M. Grundmann, and D. Bimberg, Phys. Rev. B **55**, 9740 (1997).
[18]M. Asada, Y. Miyamoto, and Y. Suematsu, IEEE J. Quantum Electron. **22**, 1915 (1986).
[19]S. Fafard, Z. R. Wasilewski, C. N. Allen, D. Picard, M. Spanner, J. P. McCaffrey, and P. G. Piva, Phys. Rev. B **59**, 15368 (1999).
[20]E. O. Kane, J. Phys. Chem. Solids **1**, 249 (1957).
[21]C. Bock, K. H. Schmidt, U. Kunze, S. Malzer, and G. H. Döhler, Appl. Phys. Lett. **82**, 2071 (2003).
[22]*Landolt-Börnstein New Series*, Vol. III/22a edited by O. Madelung, W. von der Osten, and U. Rossler (Springer, Berlin, 1987).